## Research Article

# Eco-Friendly Synthesis of Aluminium Nanoparticles from Rice Straw Extract: A Novel Approach to Combat Antimicrobial Resistance in *Staphylococcus aureus* and *Escherichia coli*

**[1,2*]Mathew Gideon, [1]Nathan Aliyu Dikko**

[1,] Department of Pure and Applied Chemistry, Faculty of Physical Science Kaduna State University, Kaduna, Nigeria.

[2,] Department of Environment, Ministry of Environment and Natural Resources, Kaduna State, Nigeria.

*Corresponding Author E-mail: mathewace8@gmail.com, https://orcid.org/0000-0002-9269-9722

**ABSTRACT**

This study presents an eco-friendly synthesis of aluminium nanoparticles (AlNPs) using rice straw extract (*Rs*-AlNPs) to address antimicrobial resistance. ATR-FTIR spectroscopy indicated the reduction and involvement of hydroxyl, alkane, overtone, and carbonyl groups in nanoparticle formation, evidenced by the disappearance of characteristic peaks. SEM analysis revealed *Rs*-AlNPs with an average diameter of 70-103 nm, predominantly spherical with slight agglomeration. EDX analysis confirmed aluminium as the predominant element (49.11%) with significant contributions from potassium (24.99%), magnesium (11.26%), and silicon (6.82%), consistent with rice straw composition. XRD analysis identified microcline (42%), enstatite (21%), quartz HP (16%), and osumilite (20%) as major crystalline phases, indicating a high aluminium content. Antimicrobial tests demonstrated dose-dependent efficacy against *Staphylococcus aureus* and *Escherichia coli.* For *S. aureus,* inhibition zones increased from 8.0 mm at 50 µg to 16.0 mm at 100 µg, while for *E. coli*, zones increased from 2.0 mm at 25 µg to 14.8 mm at 100 µg. These findings underscore the potential of Rs-AlNPs as effective antimicrobial agents and highlight a sustainable approach to nanoparticle synthesis using agricultural waste, offering a viable solution to combat antimicrobial resistance.

**KEYWORDS:** Aluminium nanoparticles (AlNPs), Rice straw extract, Antimicrobial resistance, Staphylococcus aureus, Escherichia coli, Sustainable nanotechnology, Agricultural waste utilization

## 1.0 INTRODUCTION

Recent advancements in the field of metal oxide nanoparticles (MONPs) have revolutionized their application in medicine, particularly in targeted drug delivery, imaging techniques, and antimicrobial treatments. These nanoparticles, ranging from 1 to 100 nanometers in size, possess unique physical and chemical properties due to their high surface area to volume ratio and quantum effects, making them highly reactive and suitable for diverse applications in medicine, electronics, and materials science (Krishnan & Shrestha, 2020; Sharma & Siskova,

2020). In medicine, MONPs are increasingly used as contrast agents in magnetic resonance imaging (MRI) to enhance image clarity and aid in early disease diagnosis. Moreover, they are integrated into wound dressings and coatings to prevent infections, leveraging their potent antimicrobial properties (Singh & Lillard Jr, 2009; Liu & Atwater, 2007). These advancements promise more effective and less invasive medical treatments.

Aluminium nanoparticles (AlNPs), in particular, have emerged as effective antibacterial agents due to their high surface area to volume ratio, which enhances their interaction with bacterial cells. They generate reactive oxygen species (ROS) that damage bacterial cell walls and membranes, inhibiting bacterial growth and disrupting biofilm formation. This makes them invaluable in medical and industrial applications for preventing bacterial contamination (Pal & Tak, 2007; Rai & Yadav, 2009). Recent innovations in the green synthesis of aluminium oxide and aluminium nanoparticles using plant extracts have garnered attention for their eco-friendly nature and potential biomedical applications. Various plant extracts, such as Aloe vera, green tea, neem leaf, and turmeric rhizome, have been utilized as reducing agents and stabilizers in the synthesis process, resulting in nanoparticles with controlled sizes and enhanced antimicrobial and antioxidant properties (Rajeswari & Jayalakshmi, 2016; Pandey & Goswami, 2018; Arora, Sharma, & Jyoti, 2019; Hemmati *et al.*, 2020). For instance, Aloe vera extract has been successfully employed to reduce aluminium ions, leading to the synthesis of aluminium oxide nanoparticles with significant antimicrobial activity against pathogens like *E. coli* and *S. aureus* (Rajeswari & Jayalakshmi, 2016). Similarly, green tea extract has shown promise in producing aluminium nanoparticles with antioxidant properties suitable for biomedical applications (Hemmati *et al.*, 2020).

Aluminium nanoparticles demonstrate multifaceted properties in various biomedical applications. They enhance drug delivery in anticancer therapies, induce cytotoxicity in cancer cells, and exhibit antibacterial, anti-inflammatory, antifungal, and tissue regeneration capabilities. These properties underscore their versatility in addressing diverse medical challenges (Jain, 2005; Oliveira & Andrade, 2020). Despite these advancements, there are significant environmental challenges associated with conventional agricultural practices, particularly the disposal of agricultural residues. These residues, comprising organic materials such as crop stalks, husks, and seeds, contribute to greenhouse gas emissions and environmental degradation when improperly managed (Smith OB, 1987). Agricultural residues are often burned indiscriminately, exacerbating air pollution and contributing to climate change through increased carbon emissions (Adeoye *et al.*, 2011; Simonyan, & Fasina,2013; Oladipo *et al.*, 2017; Mojisola, 2023)

This practice not only harms the environment but also poses health risks due to the inhalation of toxic fumes. To mitigate these environmental impacts, researchers are exploring innovative approaches such as utilizing agricultural residues in the synthesis of nanoparticles. This approach aligns with the principles of green chemistry by reducing reliance on hazardous chemicals and energy-intensive processes, thus promoting sustainability (Pandey & Goswami, 2018). The use of agricultural residues, like rice straw, in nanoparticle synthesis presents an opportunity to convert waste into valuable materials. Research focusing on the synthesis of aluminium nanoparticles from rice straw extract under slightly acidic to neutral pH conditions aims to evaluate their antimicrobial efficacy against drug-resistant strains of bacteria.

This study not only seeks to provide an eco-friendly and cost-effective approach to nanoparticle synthesis but also addresses the pressing issue of antimicrobial resistance. By leveraging underutilized agricultural residues, such as

rice straw, this research aims to develop nanoparticles with enhanced antimicrobial properties against pathogens like *Staphylococcus aureus* and *Escherichia coli*. The integration of green synthesis methods using plant extracts and agricultural residues underscores a shift towards sustainable practices in nanoparticle production, offering promising solutions to global health and environmental challenges.

## 2.0 MATERIALS AND METHODS

### 2.1 Materials

The experimental materials included aluminium chloride $AlCl_3$, Tetraoxosulphate (VI) Acid $H_2SO_4$, Mueller-Hinton Agar (MHA), deionized water, an analytical balance, petri dishes, antimicrobial discs, S. aureus and E. coli isolates, a magnetic stirrer, a centrifuge (KA-1000), SEM-EDX equipment, NLNG, ATR-FTIR (Agilent Cary 630 FTIR), UV-Vis (Agilent Cary 5000 UV-Vis-NIR spectrophotometer), an XRD machine, and an incubator.

### 2.2 Sampling

Rice straw was harvested from a fadama near Oil Village, Kaduna Refining and Petrochemical Company (KRPC). Analytical grade aluminium chloride and sulphuric acid were sourced from the Department of Chemistry Laboratory, Kaduna State University. Drug-resistant strains of *Staphylococcus aureus* and *Escherichia coli* were isolated and characterized at the Chemical Pathology, Haematology, and Microbiology Diagnostic Laboratory of Oxford Hospital, Makera, Kakuri, Kaduna State, Nigeria.

### 2.3 Preparation of Precursor ($AlCl_3$) and Plant Extract

Following the method by Mamman *et al.* (2024) with slight modifications, 3.33 g of aluminium chloride ($AlCl_3$) were accurately weighed and transferred to a 100 mL volumetric flask. Approximately 70 mL of deionized water was added, and the flask was capped and shaken vigorously until the aluminium chloride dissolved completely. Deionized water was then added to bring the volume to 100 mL, and the flask was labelled with the concentration (0.25 M $AlCl_3$). For the rice straw extract preparation, collected rice straw was cleaned of contaminants, rinsed under running tap water, and dried in an oven at 60°C for 24 hours. Once dry, it was ground into a fine powder, sieved for uniformity, and 20 g of the powder was mixed with 200 mL of deionized water in a 500 mL beaker. The mixture was heated to boiled for 30-60 minutes. After cooling it was then filtered, the extract was stored for use as a capping and stabilizing agent.

### 2.4 Synthesis of $AlCl_3$ Nanoparticles

To synthesize $AlCl_3$ nanoparticles, 70 mL of the prepared aluminium chloride solution was combined with 30 mL of the rice straw extract in a 250 mL beaker. The mixture was heated on a hot plate at 60-70°C with continuous stirring. Concentrated sulphuric acid (0.1 mL) was added dropwise until the pH reached 6.2, the solution colour changed from dark brown to light brown indicates nanoparticle formation.

The mixture was left undisturbed for 24 hours to confirm nanoparticle stability. Green-synthesized rice straw-aluminium nanoparticles (*Rs*-AlNPs) were separated via centrifugation, and the collected nanoparticles were dried in an oven at 45°C. The synthesized aluminium nanoparticles were characterized using various spectroscopic techniques: Fourier Transform Infrared Spectroscopy (FTIR): ATR-FTIR (Agilent Cary 630 FTIR) was utilized to analyse functional groups and chemical bonds. Scanning Electron Microscopy with Energy-Dispersive X-ray (SEM-EDX) was employed to examine nanoparticle morphology and elemental composition. X-ray Diffraction

(XRD) analysis was conducted to identify nanoparticle crystalline structure and phase purity. These characterization techniques provided comprehensive insights into the formation, morphology, and composition of aluminium nanoparticles synthesized using the green approach with rice straw extract.

## 2.5 Characterization of *Rs*-AlNPs synthesized nanoparticles.

The synthesis of green-synthesized *Rs*-AlNPs was characterized using advanced analytical techniques at the Multiuser Laboratory of the Chemistry Department, Faculty of Physical Sciences, Ahmadu Bello University, Zaria, Kaduna, Nigeria.

For Fourier Transform Infrared Spectroscopy (FTIR) analysis, an Agilent ATR-FTIR instrument was utilized following calibration procedures. The instrument parameters included a sample scan of 30 and a background scan of 16, operating over a range from 4000 $cm^{-1}$ to 650 $cm^{-1}$ with a resolution set at 8. After placing a small amount of the sample onto the ATR crystal surface and ensuring direct contact, infrared spectra were collected. This method enabled the identification of functional groups within rice straw extracts and the synthesized nanoparticles, respectively (Yilleng *et al.,* 2020; Mathew, 2023; Mamman *et al.*, 2024).

Scanning Electron Microscopy (SEM) was employed to examine *Rs*-AlNPs, the nanoparticle was dispersed on a suitable substrate. The SEM apparatus parameters, such as accelerating voltage, working distance, and beam current, were adjusted for optimal imaging. The electron beam was precisely aligned with the sample, and SEM images were captured to visualize the morphology and surface characteristics of the *Rs*-AlNPs (Mamman *et al.,* 2024).

Energy Dispersive X-ray (EDX) analysis followed SEM imaging, where the EDX mode was activated with careful detector configuration. Regions of interest were designated on SEM images to facilitate element identification and quantification of their relative abundance. EDX spectra were analysed using specialized software to determine elemental composition. Results were correlated with SEM images to elucidate the elemental distribution on the surface of *Rs*-AlNPs (Mamman *et al.*, 2024).

X-ray Diffraction (XRD) analysis involved dispersing finely ground *Rs*-AlNPs in a suitable medium to create a thin film. This film was then placed on a sample holder, such as a glass slide or silicon wafer. The X-ray diffractometer was calibrated using a standard reference material with known crystal structure and lattice parameters. An appropriate wavelength and $2^{\theta}$ angle range of 0.00–70.0 were selected to analyse the *Rs*-AlNPs nanoparticles and determine their crystalline structure and phase composition.

This comprehensive characterization using FTIR, SEM, EDX, and XRD techniques provided detailed insights into the properties and structure of the green-synthesized nanoparticles, contributing to the understanding of their potential applications in various fields.

### 2.6 Antimicrobial Susceptibility Test of *Rs*-AlNPs on Bacteria Isolates

Escherichia coli (isolated from urine) and Staphylococcus aureus (isolated from a high vaginal swab) were isolated, characterized, and identified. These bacterial strains were cultured using the Kirby-Bauer disk diffusion method on Mueller-Hinton Agar (MHA) (*Mathew et al.,* 2023). To identify drug resistance in the bacteria isolates, high-profile positive/negative 10-tipped multiple susceptibility antibiotic discs containing various antibiotics were employed. The bacterial cultures that exhibited resistance to Amoxicillin, Septrin, Streptomycin, Ampiclox, and Chloramphenicol were selected for further testing.

These resistant strains were subsequently cultured to assess the antimicrobial activity of rice straw-aluminum nanoparticles (*Rs*-AlNPs). Two concentrations of *Rs*-AlNPs, 25 µg and 50 µg, were prepared and tested against the resistant *S. aureus* strain. Four concentrations—25 µg, 50 µg, 75 µg, and 100 µg were prepared and tested against the resistant *E. coli* strain. The Zone of Inhibition (ZOI) was measured in millimeters according to the guidelines of the Clinical and Laboratory Standards Institute (CLSI) (Daniel *et al.*, 2022), providing a quantitative measure of the antimicrobial efficacy of Rs-AlNPs against these drug-resistant bacterial strains.

# 3. Results and discussions

### 3.1 Synthesis of Aluminium Nanoparticles Using Rice Straw Extract

The synthesis of aluminium nanoparticles (AlNPs) involved combining rice straw extract with an aluminium chloride ($AlCl_3$) solution and heating the mixture at 60-70°C for 10 minutes. Acidifying the mixture with concentrated sulphuric acid induced a colour change from dark brown to light brown as depicted in figure 1, indicating successful nanoparticle formation. This change results from the Surface Plasmon Resonance (SPR) phenomenon, where conduction electrons on the nanoparticle surface resonate with incident light, confirming the presence of nanoscale particles. Electrostatic interactions and hydrogen bonding between the capping and stabilizing agents in the rice straw extract and aluminium ions also drive the synthesis process. These interactions are essential for reducing aluminium ions to nanoparticles and preventing their agglomeration by stabilizing them in the solution. The transition from dark brown to light brown during synthesis is consistent with literature findings, suggesting the reduction process completes within 24 hours (Mamman *et al.*, 2024).

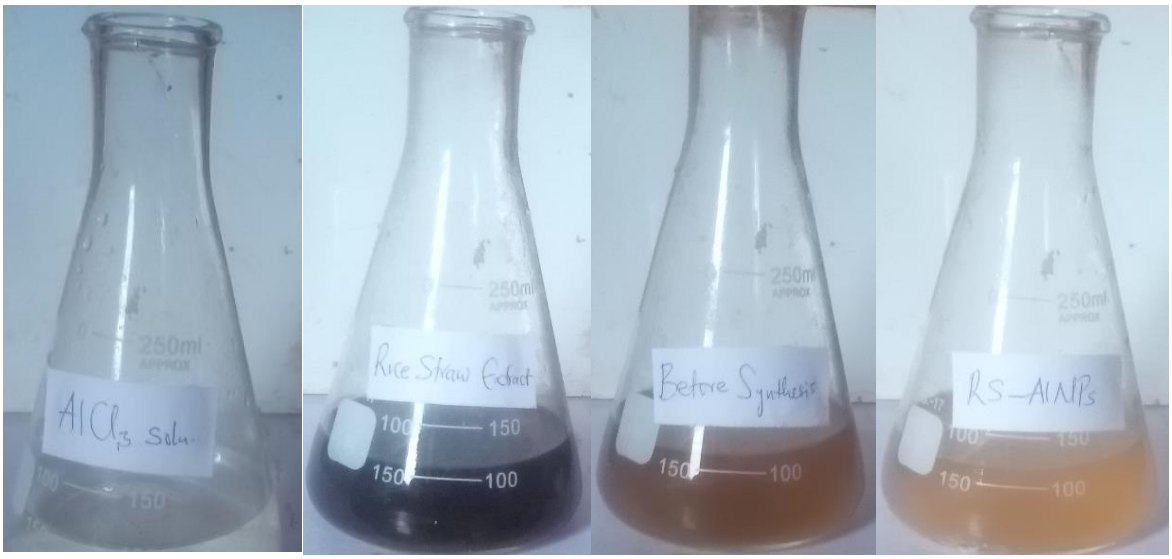


Figure 1. Colour changes in from precursor to aluminium nanoparticle synthesis

Rice straw extract serves dual roles as a reducing agent, facilitating aluminium ion reduction, and as a stabilizing agent, maintaining nanoparticle stability and dispersity. The extract's natural compounds, such as flavonoids,

polyphenols, and proteins, not only reduce aluminium ions but also provide a protective capping layer around the nanoparticles, enhancing their stability and functionality. This green synthesis method aligns with sustainable chemistry principles, reducing the need for hazardous chemicals and energy-intensive processes typical of conventional nanoparticle synthesis. By utilizing rice straw, an agricultural waste product, this approach promotes environmental sustainability and resource efficiency, creating value from waste materials (Caroling *et al.,* 2015, Yilleng *et al.,* 2020; Mamman *et al.,* 2024).

### 3.2 ATR-FTIR spectroscopy of Rice Straw extract

The synthesis of aluminium nanoparticles using rice straw extract (*Rs*-AlNPs) involves several changes in the ATR-FTIR spectra as shown in figure 2, the observable peak at 3,280.1 $cm^{-1}$ is generally attributed to O-H stretching vibrations, commonly found in alcohols and phenols, the peaks 2,922.2 $cm^{-1}$ and 2,855.1 $cm^{-1}$ correspond to C-H stretching vibrations in alkanes, 2,113.4 $cm^{-1}$ could be attributed to C≡C stretching, indicating the presence of alkynes. The peak at 1,997.9 $cm^{-1}$ is less common but might be due to overtone or combination bands, 1,736.9 $cm^{-1}$ and 1,710.8 $cm^{-1}$ are indicative of C=O stretching vibrations, typically found in carbonyl groups (esters, aldehydes, ketones). 1,636.3 $cm^{-1}$ corresponds to C=C stretching vibrations, suggesting the presence of alkenes or aromatic rings. The peak 1,513.3 $cm^{-1}$ can be attributed to N-O asymmetric stretching in nitro compounds, 1,457.4 $cm^{-1}$ and 1,420.1 $cm^{-1}$ are related to C-H bending vibrations in alkanes, 1,375.4 $cm^{-1}$ is associated with C-H bending in alkanes, 1,319.5 $cm^{-1}$ could be related to C-N stretching vibrations in amines while 1,230.0 $cm^{-1}$ corresponds to C-O stretching in alcohols, ethers, or esters and 1,028.7 $cm^{-1}$ is often attributed to C-O-C stretching in ethers. (Iravani, 2011; Ahmed *et al.,* 2016).

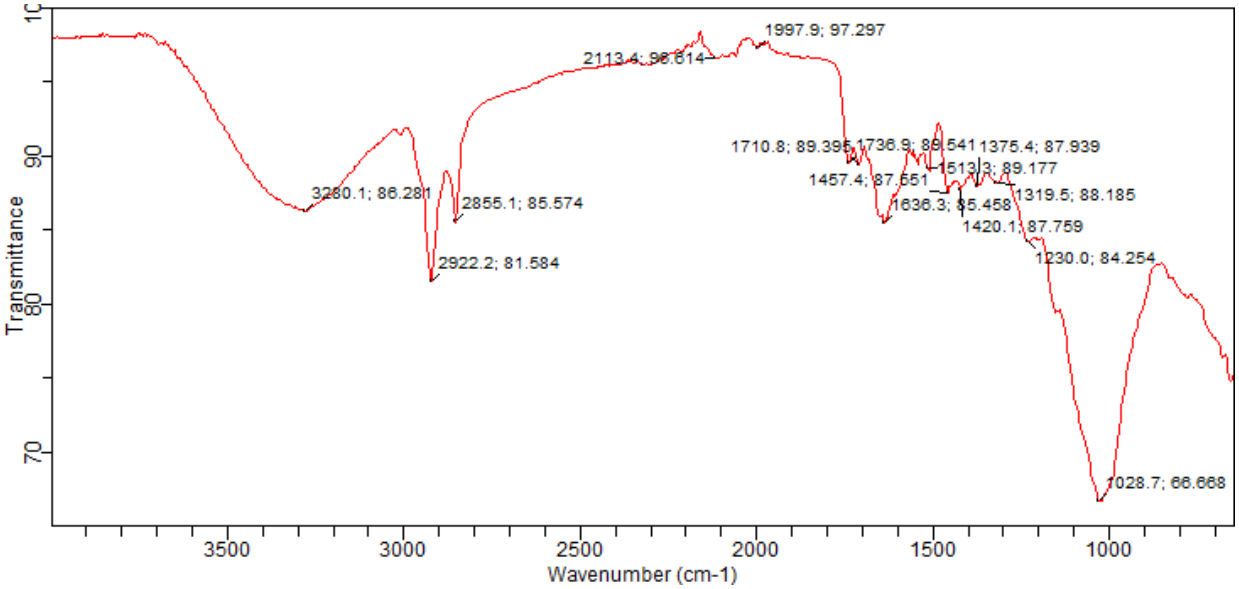

Figure 2. ATR-FTIR Spectra of Rice Straw Extract

### 3.3 ATR-FTIR spectroscopy of Aluminium nanoparticles (*Rs*-AlNPs)

The synthesis of aluminium nanoparticles using rice straw extract (*Rs*-AlNPs) involves several changes in the ATR-FTIR spectra as shown in figure 3 indicating the involvement of various functional groups in the reduction and stabilization of aluminium nanoparticles.

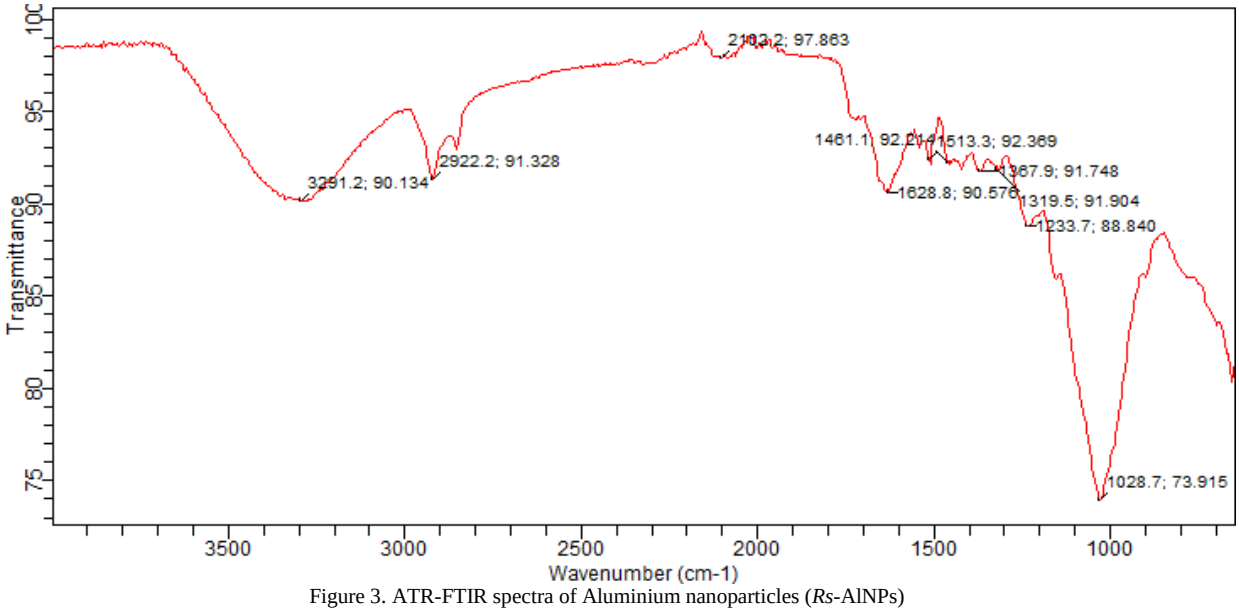

Figure 3. ATR-FTIR spectra of Aluminium nanoparticles (*Rs*-AlNPs)

The peak 3,291.2 $cm^{-1}$ slightly shifted from 3,280.1 $cm^{-1}$, still corresponds to O-H stretching, indicating the presence of alcohols or phenols, 2,922.2 $cm^{-1}$ Unchanged, indicating the presence of C-H stretching in alkanes, 2,102.2 $cm^{-1}$ slightly shifted from 2,113.4 $cm^{-1}$, suggests the continued presence of alkynes. The peak at 1,628.8 $cm^{-1}$ slightly shifted from 1,636.3 $cm^{-1}$, indicates C=C stretching, implying alkenes or aromatic rings are still present, 1,513.3 $cm^{-1}$ Unchanged, indicating N-O asymmetric stretching in nitro compounds, 1,461.1 $cm^{-1}$ also Slightly shifted from 1,457.4 $cm^{-1}$, associated with C-H bending in alkanes, 1,367.9 $cm^{-1}$ Slightly shifted from 1,375.4 $cm^{-1}$, associated with C-H bending. The peak at 1,319.5 $cm^{-1}$ remain Unchanged, indicating C-N stretching in amines. 1,233.7 $cm^{-1}$ Slightly shifted from 1,230.0 $cm^{-1}$, indicating C-O stretching in alcohols, ethers, or esters. The peak at 1,028.7 $cm^{-1}$ remain Unchanged, which corresponds to C-O-C stretching in ethers. (Sharma., et al. 2009; Thakkar et al. 2010; Mittal et al. 2013).

The peak at 3,280.1 $cm^{-1}$ Missing, suggests the reduction of hydroxyl groups during nanoparticle synthesis, 2,855.1 $cm^{-1}$ Missing, indicating the possible consumption of certain alkane groups, 1,997.9 $cm^{-1}$ Missing, could mean the disappearance of specific overtone or combination bands, the peaks at 1,736.9 $cm^{-1}$ and 1,710.8 $cm^{-1}$ Missing, could suggest the reduction or involvement of carbonyl groups (esters, aldehydes, ketones) in the formation of nanoparticles, while 1,420.1 $cm^{-1}$ Missing, indicates the possible involvement of C-H bending groups in the synthesis process. (Iravani, 2011; Ahmed *et al.*, (2016). The synthesis of *Rs*-AlNPs shows significant changes in the FTIR spectrum, indicating the involvement of various functional groups in the reduction and stabilization of aluminium nanoparticles. The disappearance of peaks related to O-H, C-H (alkanes), and carbonyl groups (C=O) suggests their participation in the reduction process, leading to the formation of Al nanoparticles. This is supported by the literature, where plant extracts rich in phenols, alcohols, and carbonyl compounds are known to act as reducing agents in nanoparticle synthesis. (Sharma *et al.*, 2009; Thakkar *et al.*, 2010; Mittal *et al.;* 2013). For example, phenolic compounds (O-H stretching) can donate electrons to reduce metal ions, forming nanoparticles and resulting in the disappearance of the corresponding FTIR peaks. Similarly, carbonyl groups

(C=O stretching) can participate in the reduction process, as observed in various green synthesis methods for metal nanoparticles. (Iravani, 2011; Ahmed *et al.*, 2016).

### 3.4 Scanning Electron Microscope (SEM) Micrographs of Synthesized (*Rs*-AlNPs)

The SEM analysis of aluminium nanoparticles synthesized using rice straw as shown in figure 4 shows that the particles have an average diameter ranging from 70 to 103 nm. The nanoparticles are predominantly spherical but exhibit a non-uniform distribution and slight agglomeration. These observations are consistent with findings in related studies and can be explained by several factors. The spherical shape of the aluminium nanoparticles is a common characteristic in biogenic synthesis. For instance, Judith *et al.* (2021) reported nearly spherical potassium nanoparticles synthesized from *Sideroxylon capiri*. Sheoran *et al.* (2021) and Ilham *et al.* (2022) also observed spherical potassium and copper nanoparticles synthesized using plant extracts. Alankrita *et al.* (2022) noted spherical silver nanoparticles synthesized with *Polyalthia longifolia* leaf extract. These studies suggest that plant extracts often lead to the formation of spherical nanoparticles due to the natural templating effect of organic molecules, which guide the nucleation and growth processes to form more energetically favourable spherical shapes. The non-uniform distribution and slight agglomeration of nanoparticles observed in the SEM images can be attributed to the variation in biological precursors. The heterogeneous nature of biological materials, such as rice straw, leads to variations in the concentration and distribution of reducing agents and stabilizing compounds. This results in a non-uniform nucleation and growth process, causing a broad size distribution and occasional agglomeration. The content of polyphenols and antioxidants in the biological precursor plays a crucial role in nanoparticle synthesis. High concentrations can lead to rapid reduction and stabilization of nanoparticles, potentially causing non-uniform distribution if the process is not well-controlled (Katka *et al.*, 2010; Judith *et al.*, 2021). Judith *et al.* (2021) also noted non-uniform distribution in the synthesis of green potassium nanoparticles.

Slight agglomeration is common when there is insufficient stabilization during the synthesis process. Biological extracts might not always provide consistent stabilizing agents, leading to partial agglomeration of the nanoparticles. This was similarly observed by Ilham *et al.* (2022) and Shweta *et al.* (2022) in their respective studies on the synthesis of nanoparticles using plant extracts. When comparing the particle sizes and shapes across different studies, some variations are noted due to differences in precursors and synthesis conditions. Aluminum nanoparticles in the current study ranged from 70 to 103 nm, were spherical, and had non-uniform distribution. Potassium nanoparticles synthesized by Judith et al. (2021) ranged from 360 to 200 nm and were spherical. Sheoran *et al.* (2021) reported potassium nanoparticles of 21 to 30 nm, also spherical. Ilham *et al.* (2022) found copper nanoparticles of 30 nm, spherical. Shweta et al. (2022) observed magnetite nanoparticles of 1 µm, with shape not specified. Alankrita *et al.* (2022) noted silver nanoparticles of less than 18 nm, spherical. These differences highlight that the specific type of plant extract, the particular polyphenols and antioxidants present, and the synthesis conditions (such as pH, temperature, and reaction time) significantly influence the final nanoparticle characteristics.

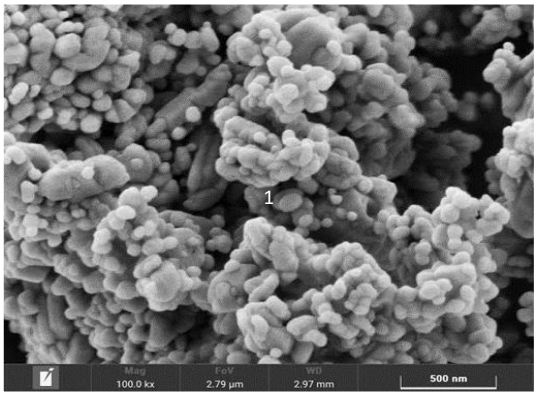


| Element | Symbol | Atomic Conc. | Weight Conc. |
|---|---|---|---|
| Aluminum | Al | 49.11 | 44.15 |
| Potassium | K | 24.99 | 32.56 |
| Magnesium | Mg | 11.26 | 9.12 |
| Silicon | Si | 6.86 | 6.39 |
| Sodium | Na | 3.37 | 2.58 |
| Calcium | Ca | 1.62 | 2.16 |
| Phosphorous | P | 1.30 | 1.34 |
| Sulfur | S | 0.93 | 0.99 |
| Chlorine | Cl | 0.60 | 0.71 |
| Titanium | Ti | 0.00 | 0.00 |
| Iron | Fe | 0.00 | 0.00 |

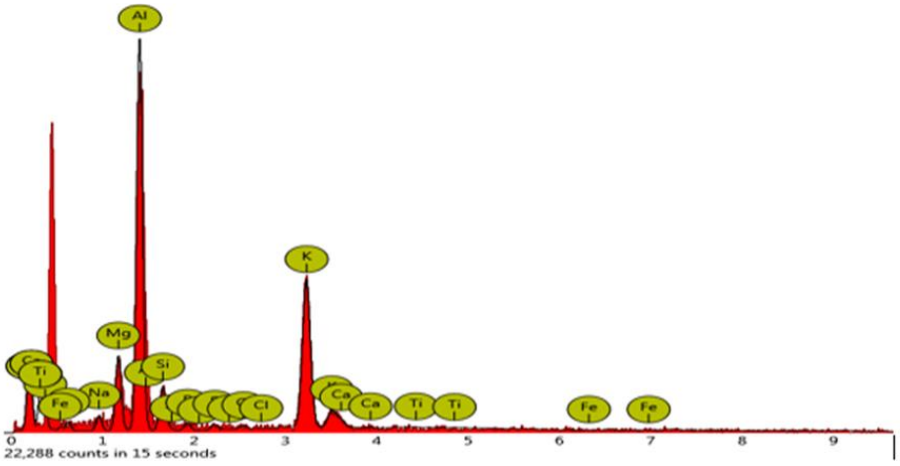


Figure 4. SEM and Energy Dispersive X-Ray (EDX) Analysis of Synthesized (*Rs*-AlNPs)

### 3.5 Energy Dispersive X-Ray (EDX) Analysis of Synthesized (*Rs*-AlNPs)

The Energy Dispersive X-ray (EDX) analysis of aluminium nanoparticles synthesized using rice straw as depicted in figure 4 indicates that aluminium (Al) is the predominant element, comprising 49.11% of the sample. Additionally, the analysis identified potassium (K), magnesium (Mg), silicon (Si), chlorine (Cl), sodium (Na), calcium (Ca), phosphorus (P), sulphur (S), iron (Fe), and titanium (Ti). The high aluminium content is expected, given that the synthesis process was specifically aimed at producing aluminium nanoparticles. The strong peak at 1.4 keV is characteristic of aluminium, confirming its significant presence. The rice straw used in the process, which contains organic materials and silica, likely acts as a reducing agent and a support matrix for the aluminium nanoparticles. The aluminium precursor used in the synthesis is the primary source of the aluminium observed in the final product. The presence of other elements, such as potassium (24.99%), magnesium (11.26%), silicon (6.82%), and trace amounts of chlorine, sodium, calcium, phosphorus, and sulphur, can be linked to the natural composition of rice straw and the synthesis process. Rice straw is known to contain various inorganic elements. Potassium is abundant in rice straw and remains in the residue after synthesis. Magnesium is present in rice straw and may also derive from additives or impurities during synthesis. The high silica content of rice straw, often up to 10-15%, accounts for the presence of silicon in the EDX results (Caroling *et al.*, 2015, Yilleng *et al.*, 2020). Chlorine, sodium, calcium, phosphorus, and sulphur are typically found in the biomass and can be incorporated into the nanoparticles or remain as residuals from the straw. Similar results were reported by Judith *et al.* (2021) in the green synthesis of potassium nanoparticles from *Sideroxylon capiri*, which showed pure potassium at 9%

and peaks of chlorine (5.33%), carbon (70.21%), and oxygen (20.38%). In a study by Sheoran *et al.* (2021) on the biogenic synthesis of potassium nanoparticles used as growth promoters in wheat, potassium sulphate was used as the precursor, resulting in a substantial potassium content of 66.72%. This higher percentage, compared to the values reported by Judith *et al.* (2021) and the present study, can be attributed to the specific potassium precursor employed by Sheoran *et al.* (2021).

### 3.6 XRD Analysis of Synthesized (*Rs*-AlNPs)

The X-ray diffraction (XRD) analysis of the *Rs*-AlNPs, as shown in Figure 5, identifies prominent peaks at diffraction angles (2θ) of 20.395°, 27.928°, 29.852°, and 41.230°. The weight fractions (wt%) from the data are: Microcline ($KAlSi_3O_8$), a potassium aluminium silicate 42%, Enstatite ($MgSiO_3$), a magnesium silicate 21%, Quartz HP ($SiO_2$), High-pressure form of silicon dioxide 16%, Osumilite ($(K,Na)_2(Fe,Mg)_2(Al,Si)_3O_{12}$) a complex aluminosilicate 20%, Lime (syn) (CaO) Calcium oxide 1.8%, Quartz (syn) ($SiO_2$) a Synthetic silicon dioxide 76.4%, Albite ($NaAlSi_3O_8$) a sodium aluminium silicate 8.33%, Orthoclase ($KAlSi_3O_8$) a potassium aluminium silicate, same as microcline but different crystal structure 14.9%, Muscovite ($KAl_2(AlSi_3O_{10})(OH)_2$) a potassium aluminium silicate hydroxide 0.4%. Microcline, with a weight fraction of 42%, is the predominant phase in the sample. This high percentage of microcline is indicative of its substantial aluminium content, which aligns with the EDX analysis showing a high aluminium concentration (49.11%) and a strong peak at 1.4 keV. This suggests a significant presence of aluminium in the synthesized nanoparticles.

The EDX analysis results, which identified aluminium as the major component, are consistent with the XRD findings, where aluminium-bearing minerals like microcline and orthoclase are significant. The strong EDX peak at 1.4 keV, characteristic of aluminium, supports the XRD results indicating that microcline ($KAlSi_3O_8$) and orthoclase ($KAlSi_3O_8$) are key constituents due to their aluminium content. A similar study by Kolawole et al. (2018) on the synthesis and characterization of cassava bark nanoparticles (CBNPs) using ball milling also identified the presence of compounds such as $SiO_2$, $CaCO_3$, $Al_2O_3$, $Ca_3SiO_5$, and $KAlSi_3O_8$. The detection of KAlSi3O8 (microcline/orthoclase) in their research corroborates the findings in this study, suggesting that aluminium-bearing silicates are common products in the synthesis of nanoparticles using plant-based materials.

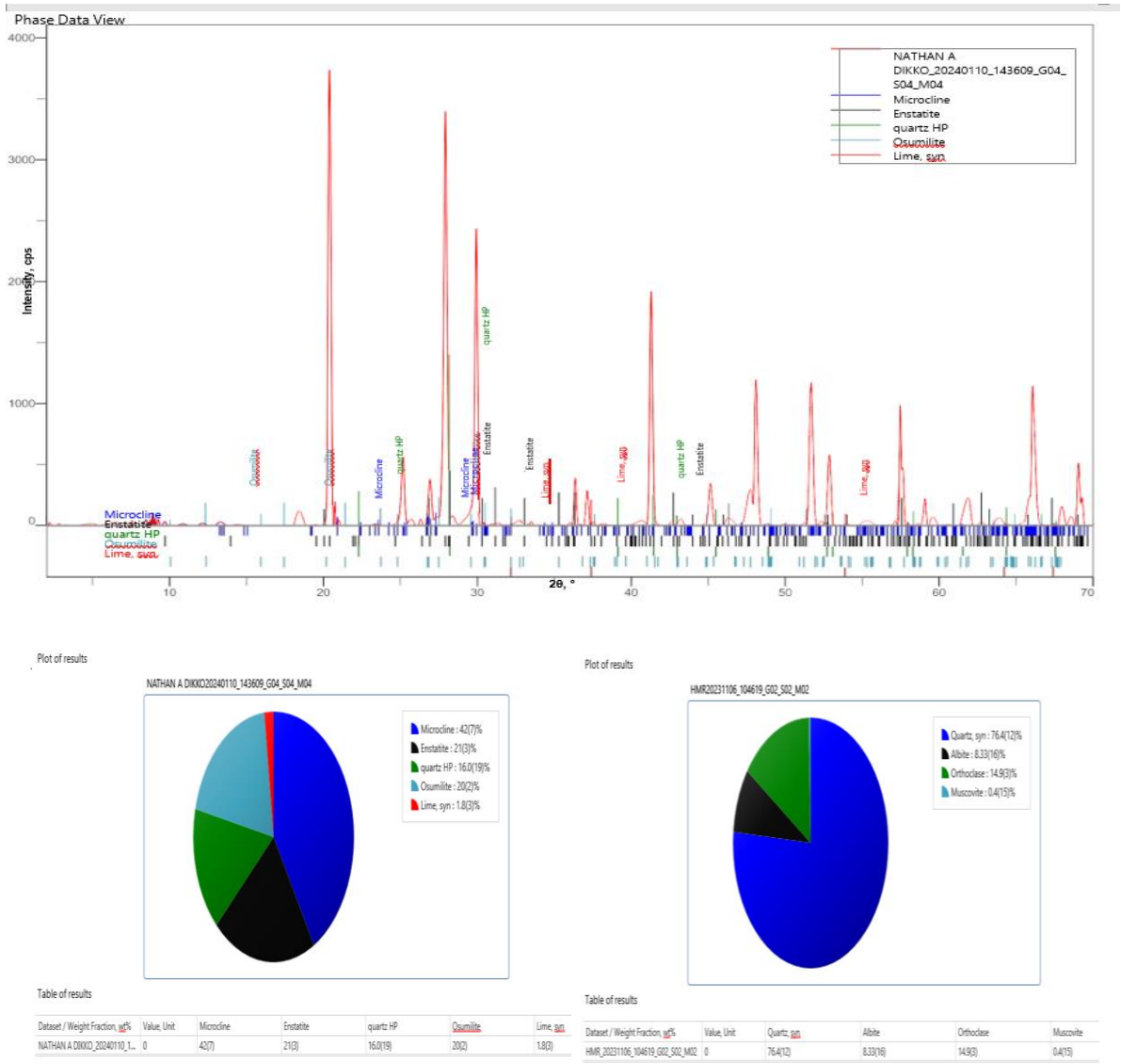


Figure 5. XRD Analysis of Synthesized (*Rs*-AlNPs)

### 3.7 Antimicrobial Susceptibility Test of *Rs*-AlNPs

Table 1 and figure 6 presents the antibacterial activity of Rice Straw-Aluminium Nanoparticles (*Rs*-AlNPs) against *Staphylococcus aureus* and *Escherichia coli* at different concentrations, indicated by the diameter of the inhibition zones.

Table 1.0. Inhibition Zones of *Rs*-AlNPs on *S. Aureus* and *E. coli* at different concentration

| **Bacteria** | ***S. Aureus*** | | ***E. Coli*** | | | |
|---|---|---|---|---|---|---|
| **Concentration** | 50 µg | 100 µg | 25 µg | 50 µg | 75 µg | 100 µg |
| **Inhibition Zone Diameter** | 8.0 mm | 16.0 mm | 2.0 mm | 6.0 mm | 11 mm | 14.8 mm |

For *Staphylococcus aureus*, at a concentration of 50 µg, the inhibition zone measures 8.0 mm, which significantly increases to 16.0 mm at a concentration of 100 µg. This indicates a substantial jump in antibacterial activity at higher concentrations. In the case of *Escherichia coli*, at a concentration of 25 µg, the inhibition zone is 2.0 mm. This increases to 6.0 mm at 50 µg, further to 11.0 mm at 75 µg, and reaches 14.8 mm at 100 µg. These results show a more gradual and consistent increase in antibacterial activity with rising concentrations of *Rs*-AlNPs.

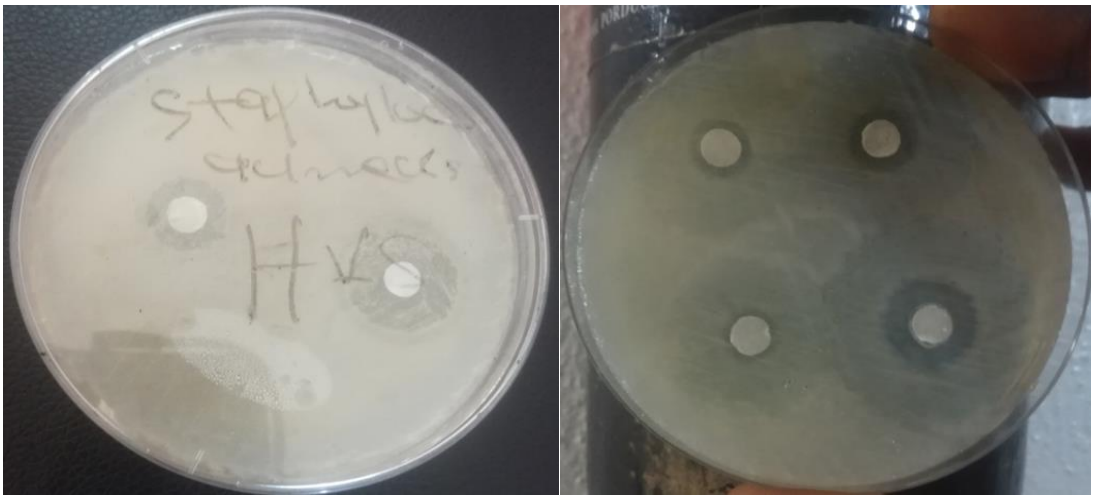

Figure 6. Antimicrobial disc of *Rs*-AlNPs on *S. Aureus* and *E. coli*

Comparatively, *E. coli* demonstrates a more predictable and linear increase in inhibition zone diameter as the concentration of nanoparticles increases. In contrast, *S. aureus* exhibits intermediate susceptibility with a less predictable pattern of inhibition zone growth, particularly noting the significant increase between 50 µg and 100 µg concentrations. Similar studies support these findings. Shrivastava *et al.* (2007) found that biosynthesized silver nanoparticles showed more pronounced antibacterial activity against *E. coli* than *S. aureus*, which is consistent with the observed larger and more consistent inhibition zones for *E. coli*. Ahmed et al. (2016) reported similar trends with biosynthesized gold nanoparticles, where *E. coli* was more susceptible than *S. aureus*. Ahamed *et al.* (2013) noted that biosynthesized copper oxide nanoparticles had greater antibacterial effects on *E. coli* than on *S. aureus*, suggesting structural differences in the cell walls of Gram-negative and Gram-positive bacteria as a possible reason. Raghupathi *et al.* (2011) observed that biosynthesized zinc oxide nanoparticles produced more significant inhibition zones in *E. coli* compared to *S. aureus*, reinforcing the pattern that *E. coli*, a Gram-negative bacterium, is generally more susceptible to nanoparticle-induced antibacterial activity compared to *S. aureus*, a Gram-positive bacterium.

## 4.0 CONCLUSION

The synthesis of aluminium nanoparticles (AlNPs) using rice straw extract offers a promising solution to antimicrobial resistance and sustainable nanomaterial production. This study has demonstrated the viability of using an eco-friendly and cost-effective method to produce AlNPs with potent antimicrobial properties by utilizing agricultural residues like rice straw. ATR-FTIR results showed significant changes in functional groups during *Rs*-AlNPs synthesis. Disappearance of peaks at 3,280.1 $cm^{-1}$, 2,855.1 $cm^{-1}$, 1,997.9 $cm^{-1}$, 1,736.9 $cm^{-1}$, 1,710.8 $cm^{-1}$, and 1,420.1 $cm^{-1}$ indicates the reduction and involvement of hydroxyl, alkane, overtone, carbonyl, and C-

H bending groups, respectively. These functional groups are crucial in the reduction and stabilization of aluminium nanoparticles. SEM micrographs revealed that the synthesized *Rs*-AlNPs are predominantly spherical with an average diameter of 70 to 103 nm. The particles exhibited non-uniform distribution and slight agglomeration, typical in green synthesis due to the variability of organic compounds in plant extracts. EDX analysis confirmed that aluminium is the predominant element in the nanoparticles, comprising 49.11% of the sample with a strong peak at 1.4 keV. Other elements present include potassium (24.99%), magnesium (11.26%), and silicon (6.82%), attributed to the natural composition of rice straw and its role in the synthesis process. XRD patterns identified several crystalline phases in *Rs*-AlNPs, with microcline (KAlSi3O8) being the most prominent at 42%. Other phases included enstatite (21%), quartz HP (16%), and osumilite (20%), aligning with EDX findings and supporting the substantial aluminium content in the nanoparticles. The antibacterial efficacy of *Rs*-AlNPs was significant and concentration-dependent. For *Staphylococcus aureus*, the inhibition zone increased from 8.0 mm at 50 µg to 16.0 mm at 100 µg, indicating heightened antibacterial activity at higher concentrations. For *Escherichia coli,* the inhibition zone grew from 2.0 mm at 25 µg to 14.8 mm at 100 µg, showing a predictable and linear increase in antimicrobial efficacy.

This study underscores the potential of rice straw, an agricultural residue, as a valuable resource for the green synthesis of aluminium nanoparticles. The significant antimicrobial properties of *Rs*-AlNPs against both Staphylococcus aureus and Escherichia coli highlight their potential application in combating antibiotic-resistant pathogens.

**Acknowledgments**

The authors express gratitude to Mr. Samuel of the Department of Chemical Pathology, Haematology, and Microbiology Diagnostic Laboratory at Oxford Hospital Makera, Kakuri, Kaduna State, Nigeria. His assistance in the antimicrobial analysis was invaluable to the success of this research.

**Legal ethics**

The study obtained ethical approval from the Ministry of Health in Kaduna State, Nigeria. Adherence to ethical guidelines was strictly observed, starting from the sampling of clinical isolates to the antimicrobial testing.

**Funding**

No external funding was received for this research.

**Conflict of interest**

The authors declare that they have no competing financial interests.

## REFERENCES

Adeoye, P., Aderemi, A., Segun, E., & Musa, J. J. (2011). Agricultural Post-Harvest Waste Generation and Management for Selected Crops in Minna, Niger State, North Central Nigeria. *Journal of Applied Sciences in Environmental Sanitation*, 6(4), 427-435.

Ahmed, S., et al. (2016). Green synthesis of silver nanoparticles using Azadirachta indica aqueous leaf extract. *Journal of Radiation Research and Applied Sciences*, 9(1), 1-7.

Arora, S., Sharma, J., & Jyoti, K. (2019). Green synthesis of aluminium nanoparticles using Curcuma longa (turmeric) rhizome extract: Characterization and biomedical applications. *Journal of Molecular Liquids*, 278, 224-230. DOI: 10.1016/j.molliq.2018.11.083

Caroling, G., Nithya, P. E., Vinodhini, M., Mercy, R. A., & Shanthi, P. (2015). *Int. J. Pharm. Bio. Sci.*, 5, 25-43.

Daniel, M. W., Meghan, A. W., & Carey-Ann, D. B. (2022). Stop waiting for tomorrow: Disk diffusion performed on early growth is an accurate method for antimicrobial susceptibility testing with reduced turnaround time. *Journal of Clinical Microbiology*, 60(5).

Hemmati, S., Rashtiani, A., & Javadzadeh, Y. (2020). Green synthesis of aluminium nanoparticles using green tea extract and evaluation of their antioxidant activity. *Journal of Cluster Science*, 31, 117-125. DOI: 10.1007/s10876-019-01657-6

Iravani, S. (2011). Green synthesis of metal nanoparticles using plants. *Green Chemistry*, 13(10), 2638-2650.

Jain, K. K. (2005). Nanotechnology in clinical laboratory diagnostics. *Clinica Chimica Acta*, 358(1-2), 37-54. DOI: 10.1016/j.cccn.2005.02.026

Javed, R., Zia, M., Naz, S., Aisida, S. O., ul Ain, N., & Ao, Q. (2020). Role of Capping Agents in the Application of Nanoparticles in Biomedicine and Environmental Remediation: Recent Trends and Future Prospects. *Journal of Nanobiotechnology*, 18(1), 1–15.

Krishnan, A., & Shrestha, M. (2020). Understanding the diverse applications of nanoparticles in medicine and technology. *Journal of Nanomedicine & Nanotechnology*, 11(2), 273-288. DOI: 10.4172/2157-7439.1000535

Liu, X., & Atwater, M. (2007). Metal oxide nanoparticles in medical imaging: Synthesis and applications. *International Journal of Biomedical Imaging*, 2007, 1-9. DOI: 10.1155/2007/86819

Mamman, A. J., Bako, M., & Zakari, L. (2024). Antimicrobial Activity of Green Synthesized Copper Nanoparticles (CuNPs) Using Aqueous Extract of Psidium guajava on Clinical Bacteria Isolates. *Fine Chemical Engineering*, 5(1), 123. DOI: https://doi.org/10.37256/fce.5120244078

Marișca, O. T., & Leopold, N. (2019). Anisotropic Gold Nanoparticle-Cell Interactions Mediated by Collagen. *Materials*, 12(7), 1131.

Mathew, G. (2023). Novel strategy for optimizing the antimicrobial activity of Psidium guajava against clinical isolates of Escherichia coli, Staphylococcus aureus, Salmonella spp., and Streptococcus spp. *INNOSC Theranostics and Pharmacological Sciences*, 5(1), 27-34.

Mathew, G., Zakari, L., Emmanuel, K. D., Mamman, A. J., & Samuel, D. (2023). Stimulating Antimicrobial Activity in Aspirin with Psidium guajava and Syzygium aromaticum Extracts against Multi-drug Resistant Salmonella Spp: A Comparative Study of Multiple Combinations. *Fine Chemical Engineering*, 4(1), 47.

Mittal, A. K., et al. (2013). Synthesis of metallic nanoparticles using plant extracts. *Biotechnology Advances*, 31(2), 346-356.

Mojisola, K. Sustainable Development Agriculture: How to ensure sustainable management of agricultural wastes. [URL]. (Accessed May 2024).

Oladipo, F. O., Olorunfemi, O. D., Adetoro, O. D., & Oladele, T. O. (2017). Farm waste utilization among farmers in Irepodun Local Government Area, Kwara State, Nigeria: Implication for extension education service delivery. *Ruhuna Journal of Science*, 8, 1-11. DOI: http://doi.org/10.4038/rjs.v8i1.22.

Oliveira, L. M., & Andrade, L. N. (2020). Aluminium nanoparticles in antiulcer treatments: a review of recent advances. *Journal of Biomedical Nanotechnology*, 16(8), 1155-1171. DOI: 10.1166/jbn.2020.3045

Pal, S., & Tak, Y. K. (2007). Silver nanoparticles as an antibacterial agent: a case study on E. coli as a model for Gram-negative bacteria. *Journal of Colloid and Interface Science*, 275(1), 177-182. DOI: 10.1016/j.jcis.2004.12.010

Pandey, S., & Goswami, G. K. (2018). Green synthesis of aluminium nanoparticles using neem (Azadirachta indica) leaf extract and their antibacterial activity against Gram-positive and Gram-negative bacteria. *Microbial Pathogenesis*, 116, 215-220. DOI: 10.1016/j.micpath.2018.01.008

Parveen, S., Misra, R., & Sahoo, S. K. (2012). Green synthesis and characterization of silver and aluminium oxide nanoparticles using Azadirachta indica (neem) leaf extract. *BioNanoScience*, 2(4), 325-331. DOI: 10.1007/s12668-012-0056-7

Rajeswari, A., & Jayalakshmi, M. (2016). Green synthesis of aluminium oxide nanoparticles using Aloe vera leaf extract and its antibacterial activity against pathogens. *Journal of Pharmacy Research*, 10(2), 86-92. DOI: 10.1016/j.jopr.2015.11.003

Rai, M., & Yadav, A. (2009). Silver nanoparticles as a new generation of antimicrobials. *Biotechnology Advances*, 27(1), 76-83. DOI: 10.1016/j.biotechadv.2008.09.002

Sharma, V. K., & Siskova, K. M. (2020). Quantum effects and high surface area: The magic of nanoparticles. *Nanoscience & Nanotechnology Letters*, 12(1), 45-57. DOI: 10.1166/nnl.2020.3040

Sharma, V. K., et al. (2009). Green synthesis of silver nanoparticles using Myristica fragrans (nutmeg) seed extract. *Journal of Colloid and Interface Science*, 335(1), 77-81.

Simonyan, K. J., & Fasina, O. (2013). Biomass resources and bioenergy potentials in Nigeria. *African Journal of Agricultural Research*, 8(40), 4975-4989. DOI: 10.5897/AJAR2013.6726.

Singh, R., & Lillard Jr, J. W. (2009). Nanoparticle-based targeted drug delivery. *Experimental and Molecular Pathology*, 86(3), 215-223. DOI: 10.1016/j.yexmp.2008.12.004

Smith, O. B. Utilization of crops residues in the nutrition of sheep and goats in the humid tropics of West Africa. In Atta Krah A. N. and Reynolds L. (Eds.), *Sheep and goat meat production in the humid tropics of West Africa*. Yamoussoukro 21-25 September 1987. FAO Animal Production and Health Paper.

Thakkar, K. N., et al. (2010). Biological synthesis of metallic nanoparticles. *Nanomedicine: Nanotechnology, Biology and Medicine*, 6(2), 257-262.

Yilleng, T. M., Samuel, N. Y., Stephen, D., Akande, J. A., Agendeh, Z. M., & Madaki, L. A. (2020). *Journal of Applied Science and Environmental Management*, 24, 1987-1991.